Bull Math Biol
DOI 10.1007/s11538-010-9591-7

ORIGINAL ARTICLE

Multiple Stable Periodic Oscillations in a Mathematical Model of CTL Response to HTLV-I Infection

Michael Y. Li · Hongying Shu

Received: 22 May 2010 / Accepted: 1 October 2010

Abstract Stable periodic oscillations have been shown to exist in mathematical models for the CTL response to HTLV-I infection. These periodic oscillations can be the result of mitosis of infected target $CD4^+$ cells, of a general form of response function, or of time delays in the CTL response. In this study, we show through a simple mathematical model that time delays in the CTL response process to HTLV-I infection can lead to the coexistence of multiple stable periodic solutions, which differ in amplitude and period, with their own basins of attraction. Our results imply that the dynamic interactions between the CTL immune response and HTLV-I infection are very complex, and that multi-stability in CTL response dynamics can exist in the form of coexisting stable oscillations instead of stable equilibria. Biologically, our findings imply that different routes or initial dosages of the viral infection may lead to quantitatively and qualitatively different outcomes.

Keywords In-host models · HTLV-I infection · CTL response · Time delays · Hopf bifurcation · Multiple stable periodic solutions

1 Introduction

Human T-cell leukemia virus type I (HTLV-I) is etiologically linked to a progressive neurologic disease HTLV-I associated myelopathy/tropical spastic paraparesis

M.Y. Li (✉) · H. Shu
Department of Mathematics, Harbin Institute of Technology, Harbin, Heilongjiang 150001, P.R. China
e-mail: mli@math.ualberta.ca

M.Y. Li · H. Shu
Department of Mathematical and Statistical Sciences, University of Alberta, Edmonton, Alberta T6G 2G1, Canada

Published online: 26 October 2010

(HAM/TSP) and adult T-cell leukemia (ATL) (Kubota et al. 2000; Gallo 2005). Approximately 20 to 40 million people are infected by HTLV-I worldwide. Majority of HTLV-I infected individuals remain lifelong asymptomatic carriers, and approximately 0.25–3.8% of infected individuals develop HAM/TSP and another 2–3% develop ATL (Hollsberg and Hafler 1993; Bangham 2000). In the peripheral blood, HTLV-I primarily targets $CD4^+$ helper T cells (Bangham 2000; Jacobson 2002). HTLV-I infection in vivo is achieved through cell-to-cell contact among healthy and infected $CD4^+$ T cells, and viral materials are passed between cells through virological synapses (Bangham 2003). The HTLV-I infection elicits a strong cytotoxic T-lymphocyte (CTL) response (Bangham 2000; Jacobson 2002). On the one hand, CTL has a protective role by regulating the proviral load, and on the other, evidence suggests that cytotoxicity of the CTL is ultimately responsible for the demyelination of the central nervous system (CNS), resulting in HAM/TSP (Bangham 2000; Jacobson 2002). Investigating the interaction between the HTLV-I infection and HTLV-I-specific CTL response is important for understanding the pathogenesis of HTLV-I-related diseases and for designing therapeutic measures.

A standard mathematical model for the HTLV-I infection with CTL response can be derived by considering three compartments of cells in the peripheral blood: the uninfected $CD4^+$ target cells x, infected $CD4^+$ target cells y, and HTLV-I-specific $CD8^+$ CTLs z, with turnover rates of d_1, d_2, and d_3, respectively. We let $x(t)$, $y(t)$, $z(t)$ denote the cell concentration of the corresponding compartment at time t. Healthy $CD4^+$ T cells are produced at a constant rate λ (Perelson and Nelson 1999). The cell-to-cell transmission of HTLV-I is customarily modelled by a bilinear incidence βxy (Perelson and Nelson 1999; Nowak and May 2000). CTL-driven elimination of infected $CD4^+$ cells can be modelled by a bilinear function γyz, where γ is the rate of CTL elimination (Wang et al. 2007; Wodarz et al. 1999). The strength of CTL response to HTLV-I infection $f(y,z)$ is assumed to be dependent on both the HTLV-I-specific CTL frequency and the proviral load. To account for the time lag incurred by a sequence of events such as antigenic activation, selection, and proliferation of the CTLs (Wang et al. 2007; Burić et al. 2001), we assume that the number (per mm^3) of CTLs produced at time t is given by $f(y(t-\tau), z(t-\tau)) = \mu y(t-\tau)z(t-\tau))$, which depends on the number of CTLs and infected target cells at time $t-\tau$, for a time lag $\tau > 0$. All parameters are assumed to be positive.

The preceding assumptions lead the following HTLV-I infection model with CTL response:

$$\begin{aligned} x'(t) &= \lambda - d_1 x(t) - \beta x(t) y(t), \\ y'(t) &= \beta x(t) y(t) - d_2 y(t) - \gamma y(t) z(t), \\ z'(t) &= \mu y(t-\tau) z(t-\tau) - d_3 z(t). \end{aligned} \tag{1}$$

Model (1) and other related models for the CTL response of HTLV-I have been developed in the literature and their temporal dynamics investigated through numerical and mathematical analysis (Nowak and May 2000; Wang et al. 2007; Wodarz et al. 1999; Burić et al. 2001; Wodarz and Bangham 2000; Gomez-Acevedo and Li 2002; Asquith and Bangham 2007; Gomez-Acevedo et al. 2010; Li and Shu 2010). Several mathematical mechanisms are shown to lead to stable periodic oscillations. It is

shown in Wodarz and Bangham (2000) that mitosis in the y compartment can give rise to Hopf bifurcations and stable periodic solutions without time delays. In Lang and Li (2010), it is shown that a sigmoidal response function can lead to stable periodic solutions without mitosis and time delays. It is shown in Wang et al. (2007), Li and Shu (2010) that the time delay can destabilize the positive steady state and lead to table periodic oscillations through Hopf bifurcations with a simple form of response function and no mitosis. In the present paper, we further investigate the impact of the time lag τ on the temporal dynamics of model (1). Using both rigorous bifurcation analysis and numerical simulations, we show that the delay can destabilize an otherwise stable positive steady state and lead to the phenomenon of stability switch: as the delay increases, the positive steady state switches between being stable and unstable for a finite number of times. Stability switches have been shown to occur in a variety of biological models with time delays (Beretta et al. 2006; Carletti and Beretta 2007; Tang and Zhou 2007; Crauste 2009). A general geometric criterion was developed in Beretta and Kuang (2002) for stability switch to occur in delayed system and was further extended in Beretta and Tang (2003). Little attention, however, has been paid in the literature to the global properties of the Hopf branches that accompany the stability switches. In this paper, we show that when stability switches occur, Hopf bifurcations can happen along two separate sequences of bifurcation points (Fig. 2), and multiple stable periodic solutions can coexist for the same value of the time delay, as the result of overlapping of multiple stable Hopf branches.

Multiple periodic solutions have been shown to exist for a variety of biological models. Clark et al. (2003) established coexistence of multiple stable periodic solutions in a model for hormonal control of the menstrual cycle. Gyllenberg and Yan (2009) showed the coexistence of four limit cycles for a three-dimensional competitive Lotka–Volterra system. Hofbauer and So (1990, 1994) proved coexistence of multiple limit cycles for predator–prey models and three-dimensional Lotka–Volterra systems. Pilyugin and Waltman (2003) showed coexistence of multiple limit cycles in a chemostat model with variable yield. Our result in the present paper is the first to show that multiple stable periodic solutions can coexist in an in-host viral model. Because of the simple and standard form of model (1), we believe that the mechanism discovered in present paper is generic and robust, and may hold for more realistic and complex models, as well as for in-host models of other type of viral infections.

In the next section, we derive two threshold parameters R_0 and R_1, whose values determine the number of equilibria. Stability switches at the positive (HAM/TSP) equilibrium P_2 and the occurrence of local Hopf bifurcations are investigated in Sect. 3. Numerical evidence is given in Sect. 4 to demonstrate global properties of Hopf branches and coexistence of stable periodic solutions. Biological implications of our results and further discussions are given in Sect. 5.

2 Preliminaries

The dynamics of system (1) will be investigated in a suitable phase space and a bounded feasible region. For $\tau > 0$, denote by $\mathcal{C} = C([-\tau, 0], \mathbb{R})$ the Banach space of continuous real-valued functions on the interval $[-\tau, 0]$, with norm $\|\phi\| =$

$\sup_{-\tau\le\theta\le 0}|\phi(\theta)|$ for $\phi\in\mathcal{C}$. The nonnegative cone of $\mathcal{C}$ is $\mathcal{C}^+=C([-\tau,0],\mathbb{R}_+)$. Initial conditions for system (1) will be chosen for $t=0$ as

$$\varphi\in\mathbb{R}_+\times\mathcal{C}^+\times\mathcal{C}^+,\quad \varphi(0)>0. \tag{2}$$

The following result establishes the feasible region of the model and shows that the model is well-posed.

Proposition 2.1 *Under initial conditions in* (2), *all solutions of system* (1) *are positive and ultimately bounded in* $\mathbb{R}\times\mathcal{C}\times\mathcal{C}$. *Furthermore, all solutions eventually enter and remain in the following bounded and positively invariant region*:

$$\Gamma=\left\{(x,y,v)\in\mathbb{R}_+\times\mathcal{C}^+\times\mathcal{C}^+ : |x|\le\frac{\lambda}{d_1},\ \|x+y\|\le\frac{\lambda}{\widetilde{d}},\ \|x+y+\frac{\gamma}{\mu}z\|\le\frac{\lambda}{d}\right\},$$

where $d=\min\{d_1,d_2,d_3\}>0$ *and* $\widetilde{d}=\min\{d_1,d_2\}>0$.

Proof First, we prove that $x(t)$ is positive for $t\ge 0$. Assuming the contrary and letting $t_1>0$ be the first time such that $x(t_1)=0$, by the first equation of system (1), we have $x'(t_1)=\lambda>0$, and hence $x(t)<0$ for $t\in(t_1-\epsilon,t_1)$ and sufficiently small $\epsilon>0$. This contradicts $x(t)>0$ for $t\in[0,t_1)$. It follows that $x(t)>0$ for $t>0$ as long as $x(t)$ exists. From the second equation of (1) we have

$$y(t)=y(0)e^{\int_0^t(\beta x(\theta)-d_2-\gamma z(\theta))d\theta}.$$

It follows that $y(t)>0$ for $t>0$. Similarly we can show that $z(t)>0$ for $t>0$.

Next we show that positive solutions of (1) are ultimately uniformly bounded for $t\ge 0$. From the first equation of (1), we obtain $x'(t)\le\lambda-d_1x(t)$, and thus $\limsup_{t\to\infty}x(t)\le\frac{\lambda}{d_1}$. Adding the first two equations of (1) we get

$$\begin{aligned}(x(t)+y(t))'&=\lambda-d_1x(t)-d_2y(t)-\gamma y(t)z(t)\\&\le\lambda-\widetilde{d}(x(t)+y(t)),\end{aligned}$$

where $\widetilde{d}=\min\{d_1,d_2\}$. Thus $\limsup_{t\to\infty}(x(t)+y(t))\le\frac{\lambda}{\widetilde{d}}$. Adding all the equations of (1) we get

$$\begin{aligned}\left(x(t)+y(t)+\frac{\gamma}{\mu}z(t+\tau)\right)'&=\lambda-d_1x(t)-d_2y(t)-d_3\frac{\gamma}{\mu}z(t+\tau)\\&\le\lambda-d\left(x(t)+y(t)+\frac{\gamma}{\mu}z(t+\tau)\right),\end{aligned}$$

where $d=\min\{d_1,d_2,d_3\}$. Thus $\limsup_{t\to\infty}(x(t)+y(t)+\frac{\gamma}{\mu}z(t+\tau))\le\frac{\lambda}{d}$. Therefore, $x(t)$, $y(t)$ and $z(t)$ are ultimately uniformly bounded in $\mathbb{R}\times\mathcal{C}\times\mathcal{C}$. □

System (1) always has an infection-free equilibrium $P_0=(x_0,0,0)$, located on the boundary of Γ, where $x_0=\frac{\lambda}{d_1}$. In addition to P_0, the system can have

two chronic-infection equilibria, $P_1 = (\overline{x}, \overline{y}, 0)$ and $P_2 = (x^*, y^*, z^*)$ in Γ, where $\overline{x}$, $\overline{y}$, x^*, y^*, z^* are all positive. At equilibrium P_1, the HTLV-I infection is persistent with a constant proviral load $\bar{y} > 0$, whereas the CTL response is absent, so is the risk for developing HAM/TSP. This corresponds to the situation of an asymptotic carrier. At equilibrium P_2, both the proviral load and CTL response persist at a constant level. This corresponds to the situation of a HAM/TSP patient. The final outcome of the system is determined by a combination of two threshold parameters,

$$R_0 = \frac{\lambda\beta}{d_1 d_2}, \quad \text{and} \tag{3}$$

$$R_1 = \frac{\lambda\beta\mu}{d_1 d_2 \mu + \beta d_2 d_3}. \tag{4}$$

One can see that $R_1 < R_0$ always holds. It can be verified that the carrier equilibrium $P_1 = (\bar{x}, \bar{y}, 0)$ exists if and only if $R_0 > 1$, and that

$$\bar{x} = \frac{d_2}{\beta} = \frac{\lambda}{d_1 R_0}, \qquad \bar{y} = \frac{\lambda\beta - d_1 d_2}{\beta d_2} = \frac{d_1(R_0 - 1)}{\beta}. \tag{5}$$

The coordinates of the HAM/TSP equilibrium $P_2 = (x^*, y^*, z^*)$ are given by

$$x^* = \frac{\lambda\mu}{d_1\mu + \beta d_3} = \frac{d_2 R_1}{\beta}, \qquad y^* = \frac{d_3}{\mu},$$
$$z^* = \frac{\beta\lambda\mu - d_1 d_2 \mu - \beta d_2 d_3}{(d_1\mu + \beta d_3)\gamma} = \frac{d_1 d_2 \mu + \beta d_2 d_3}{(d_1\mu + \beta d_3)\gamma}(R_1 - 1).$$

Therefore, P_2 exists in the interior of Γ if and only if $R_1 > 1$. The following result is proved in Li and Shu (2010). For the convenience of the reader, we include the proofs in Appendix.

Theorem 2.2

(1) *If $R_0 \le 1$, then $P_0 = (\frac{\lambda}{d_1}, 0, 0)$ is the only equilibrium in Γ and it is globally asymptotically stable in Γ. The viral clearance is achieved.*
(2) *If $R_1 \le 1 < R_0$, then P_0 is unstable. The carrier equilibrium $P_1 = (\overline{x}, \overline{y}, 0)$ is the only chronic-infection equilibrium in Γ, and P_1 is globally asymptotically stable. The patient remains as an asymptotic carrier.*
(3) *If $R_1 > 1$, then P_0 and P_1 are unstable, and the HAM/TSP equilibrium $P_2 = (x^*, y^*, z^*)$ exists. Both the HTLV-I infection and the CTL response are persistent. The patient has high risk to develop HAM/TSP.*

3 Stability Switches at P_2 and Hopf Bifurcations

When $R_1 > 1$, both the HTLV-I infection and the HTLV-specific CTL response are persistent. We will further investigate the temporal dynamics of HTLV-I and CTL interaction in this case. We investigate the stability of P_2 and identify parameter regimes in which the time delay can destabilize P_2 and lead to Hopf bifurcations.

Translating the equilibrium P_2 to the origin through a change of variables $x_1(t) = x(t) - x^*$, $y_1(t) = y(t) - y^*$, $z_1(t) = z(t) - z^*$, we obtain

$$\begin{aligned} x_1'(t) &= -(\beta y^* + d_1)x_1(t) - \beta x^* y_1(t) - \beta x_1(t) y_1(t), \\ y_1'(t) &= \beta y^* x_1(t) - \gamma y^* z_1(t) + \beta x_1(t) y_1(t) - \gamma y_1(t) z_1(t), \\ z_1'(t) &= \mu z^* y_1(t-\tau) + d_3 z_1(t-\tau) - d_3 z_1(t) + \mu y_1(t-\tau) z_1(t-\tau). \end{aligned} \tag{6}$$

The characteristic equation associated with the linearization of system (6) at $(0, 0, 0)$ is

$$\xi^3 + a_2\xi^2 + a_1\xi + a_0 + (b_2\xi^2 + b_1\xi + b_0)e^{-\xi\tau} = 0, \tag{7}$$

where

$$\begin{aligned} &a_2 = d_3 + \beta y^* + d_1, \qquad a_1 = d_3(\beta y^* + d_1) + \beta^2 x^* y^*, \qquad a_0 = \beta^2 x^* y^* d_3, \\ &b_2 = -d_3, \qquad b_1 = \gamma d_3 z^* - d_3(\beta y^* + d_1), \\ &b_0 = \gamma d_3 z^*(\beta y^* + d_1) - \beta^2 x^* y^* d_3. \end{aligned}$$

When $\tau = 0$, (7) becomes

$$\xi^3 + (a_2 + b_2)\xi^2 + (a_1 + b_1)\xi + (a_0 + b_0) = 0.$$

Noticing that

$$\begin{aligned} &a_2 + b_2 = \beta y^* + d_1 > 0, \qquad a_1 + b_1 = \gamma d_3 z^* + \beta^2 x^* y^* > 0, \\ &a_0 + b_0 = \gamma d_3 z^*(\beta y^* + d_1) > 0, \\ &(a_2 + b_2)(a_1 + b_1) - (a_0 + b_0) = \beta^2 x^* y^*(\beta y^* + d_1) > 0, \end{aligned}$$

and using the Routh–Hurwitz criterion, we know that all roots of (7) with $\tau = 0$ have negative real parts. Hence we obtain the following result.

Proposition 3.1 *Suppose $R_1 > 1$. Then the HAM/TSP equilibrium P_2 of system (1) is locally asymptotically stable when $\tau = 0$.*

Time delays are known to be able to destabilize a stable equilibrium and produce oscillations. We will use the delay $\tau > 0$ as a bifurcation parameter and investigate if P_2 remains asymptotically stable or becomes unstable. Since, when $\tau = 0$, all roots of the characteristic equation (7) lie to the left of the imaginary axis, stability change at the HAM/TSP equilibrium P_2 can only occur when characteristic roots cross the imaginary axis to the right. Let $\tau > 0$ and suppose $\xi = i\omega$ $(\omega > 0)$ is a purely imaginary solution of (7). Separating the real and imaginary parts in (7), we see that ω satisfies the following equations:

$$\begin{aligned} -\omega^3 + a_1\omega &= \left(b_0 - b_2\omega^2\right)\sin\omega\tau - b_1\omega\cos\omega\tau, \\ a_2\omega^2 - a_0 &= \left(b_0 - b_2\omega^2\right)\cos\omega\tau + b_1\omega\sin\omega\tau. \end{aligned} \tag{8}$$

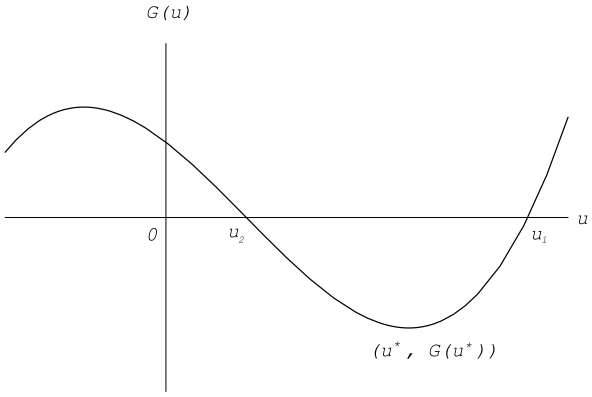

Fig. 1 Graph of $G(u)$ with two positive roots

Squaring and adding both equations of (8) leads to

$$F(\omega) = \omega^6 + \left(a_2^2 - b_2^2 - 2a_1\right)\omega^4 + \left(a_1^2 - 2a_0a_1 - b_1^2 + 2b_0b_2\right)\omega^2 + \left(a_0^2 - b_0^2\right) = 0. \quad (9)$$

Let

$$G(u) = u^3 + \left(a_2^2 - b_2^2 - 2a_1\right)u^2 + \left(a_1^2 - 2a_0a_1 - b_1^2 + 2b_0b_2\right)u + \left(a_0^2 - b_0^2\right). \quad (10)$$

Then, $i\omega$ ($\omega > 0$) is a root of (7) if and only if the equation

$$G(u) = 0$$

has a positive root $u = \omega^2$. If $G(u) = 0$ has a unique positive root, it is shown in Li and Shu (2010) that Hopf bifurcations can occur along a sequence of bifurcation values. In the following, we investigate the case when $G(u) = 0$ has exactly two positive roots. Note that

$$G'(u) = 3u^2 + 2\left(a_2^2 - b_2^2 - 2a_1\right)u + a_1^2 - 2a_0a_1 - b_1^2 + 2b_0b_2.$$

Let

$$\Delta = \left(a_2^2 - b_2^2 - 2a_1\right)^2 - 3\left(a_1^2 - 2a_0a_1 - b_1^2 + 2b_0b_2\right). \quad (11)$$

Suppose $\Delta \geq 0$. Then the graph of $G(u)$ has critical points

$$u^* = \frac{-(a_2^2 - b_2^2 - 2a_1) + \sqrt{\Delta}}{3}, \qquad u^{**} = \frac{-(a_2^2 - b_2^2 - 2a_1) - \sqrt{\Delta}}{3}. \quad (12)$$

If $u^* > 0$ and $G(u^*) < 0$, then $G(u) = 0$ has a positive root by continuity of $G(u)$. If we further assume that $G(0) = a_0^2 - b_0^2 > 0$, then $G(u) = 0$ has exactly two positive roots, $u_2 < u_1$. Furthermore, $G'(u_2) < 0$ and $G'(u_1) > 0$, see Fig. 1. We thus have the following lemma.

Lemma 3.2 *Let $G(u)$, Δ, and u^* be defined as in (10)–(12). Assume that*

(1) $a_0^2 - b_0^2 > 0$.

(2) $\Delta \geq 0$.
(3) $u^* > 0$ *and* $G(u^*) < 0$.

Then equation $G(u) = 0$ *has exactly two positive roots,* $u_2 < u_1$. *Furthermore,* $G'(u_2) < 0$ *and* $G'(u_1) > 0$.

Let $\omega_i = \sqrt{u_i}$, $i = 1, 2$. Then $\omega_2 < \omega_1$. Solving (8) for τ we obtain

$$\tau_n^{(i)} = \frac{1}{\omega_i} \arccos\left\{ \frac{(b_1 - a_2 b_2)\omega_i^4 + (a_0 b_2 + a_2 b_0 - a_1 b_1)\omega_i^2 - a_0 b_0}{(b_2\omega_i^2 - b_0)^2 + b_1^2 \omega_i^2} \right\} + \frac{2n\pi}{\omega_i},$$
$$i = 1, 2;\ n = 0, 1, 2, \ldots. \tag{13}$$

Then at two increasing sequences of τ values,

$$\tau_0^{(1)} < \tau_1^{(1)} < \cdots < \tau_n^{(1)} < \cdots, \quad \text{and}$$
$$\tau_0^{(2)} < \tau_1^{(2)} < \cdots < \tau_n^{(2)} < \cdots,$$

a pair characteristic roots cross the imaginary axis at $\pm i\omega_0$, and a local Hopf bifurcation occurs. Let

$$\tau_0 = \min\{\tau_0^{(1)}, \tau_0^{(2)}\}.$$

Then all characteristic roots of (7) have negative real parts for $\tau < \tau_0$. We thus obtain the following result.

Theorem 3.3 *Suppose that assumptions in Lemma 3.2 hold. Then*

(1) *The HAM/TSP equilibrium* P_2 *is asymptotically stable for* $\tau \in [0, \tau_0)$.
(2) *System (1) undergoes a Hopf bifurcation at the HAM/TSP equilibrium* P_2 *along two sequences of* τ *values,* $\tau_n^{(1)}$ *and* $\tau_n^{(2)}$, $n = 0, 1, 2, \ldots$.

Proof It remains to show that the transversality condition for the Hopf bifurcation theorem holds at $\tau = \tau_n^{(i)}$, $i = 1, 2$. Differentiating (7) with respective to τ we obtain

$$\left[\frac{d\xi}{d\tau}\right]^{-1} = \frac{(3\xi^2 + 2a_2\xi + a_1)e^{\xi\tau}}{\xi(b_2\xi^2 + b_1\xi + b_0)} + \frac{2b_2\xi + b_1}{\xi(b_2\xi^2 + b_1\xi + b_0)} - \frac{\tau}{\xi}.$$

Using (8) we obtain, for $i = 1, 2$, $n = 0, 1, 2, \ldots$,

$$\begin{aligned}\left[\frac{d(\mathrm{Re}\xi(\tau))}{d\tau}\right]^{-1}_{\tau=\tau_n^{(i)}} &= \mathrm{Re}\left[\frac{(3\xi^2 + 2a_2\xi + a_1)e^{\xi\tau}}{\xi(b_2\xi^2 + b_1\xi + b_0)}\right]_{\tau=\tau_n^{(i)}} \\ &\quad + \mathrm{Re}\left[\frac{2b_2\xi + b_1}{\xi(b_2\xi^2 + b_1\xi + b_0)}\right]_{\tau=\tau_n^{(i)}} \\ &= \frac{1}{b_1^2\omega_i^2 + (b_0 - b_2\omega_i^2)^2}\left\{\left(a_1 - 3\omega_i^2\right)\omega_0\left[\left(b_0 - b_2\omega_i^2\right)\sin\omega_i\tau_n^{(i)}\right.\right.\end{aligned}$$

$$
\begin{aligned}
&- b_1\omega_i \cos\omega_i\tau_n^{(i)}\big] \\
&+ 2a_2\omega_i^2\big[\big(b_0 - b_2\omega_i^2\big)\cos\omega_i\tau_n^{(i)} + b_1\omega_i \sin\omega_i\tau_n^{(i)}\big] - b_1^2\omega_i^2 \\
&+ 2b_2\omega_i^2\big(b_0 - b_2\omega_0^2\big)\big\} \\
&= \frac{3\omega_i^6 + 2(a_2^2 - b_2^2 - 2a_1)\omega_i^4 + (a_1^2 - 2a_0a_1 - b_1^2 + 2b_0b_2)\omega_i^2}{b_1^2\omega_i^4 + \omega_i^2(b_0 - b_2\omega_i^2)^2} \\
&= \frac{G'(\omega_i^2)}{b_1^2\omega_i^2 + (b_0 - b_2\omega_i^2)^2}.
\end{aligned}
$$

Since $b_1^2\omega_0^2 + (b_0 - b_2\omega_0^2)^2 > 0$, we conclude that

$$
\operatorname{sign}\left[\frac{d(\operatorname{Re}\xi(\tau))}{d\tau}\right]_{\tau=\tau_n^{(i)}} = \operatorname{sign}\left[\frac{d(\operatorname{Re}\xi(\tau))}{d\tau}\right]^{-1}_{\tau=\tau_n^{(i)}} = \operatorname{sign} G'(\omega_i^2), \quad i = 1, 2. \tag{14}
$$

Therefore, if $G'(\omega_0^2) \neq 0$, the transversality condition holds and a Hopf bifurcation occurs at $\tau = \tau_0$. This completes the proof. □

Remarks From transversality condition (14) and the fact that $G'(\omega_1^2) < 0$ and $G'(\omega_2^2) > 0$, we know the following.

(a) At each $\tau_n^{(1)}$ of the first sequence, $n = 0, 1, 2, \ldots$, a pair of characteristic roots of (7) cross the imaginary axis to the right.
(b) Along the second sequence $\tau_n^{(2)}$, $n = 0, 1, 2, \ldots$, a pair of characteristic roots of (7) cross the imaginary axis to the left.
(c) Using relations $\omega_2 = \sqrt{u_2} < \sqrt{u_1} = \omega_1$ and (13) we know that

$$
\omega_n^{(1)} - \omega_{n-1}^{(1)} = \frac{2\pi}{\omega_1} < \frac{2\pi}{\omega_2} = \omega_n^{(2)} - \omega_{n-1}^{(2)}.
$$

Therefore, there exists $k \in \mathbb{N}$ such that the two sequences, $\tau_n^{(1)}$, and $\tau_n^{(2)}$ satisfy the relation

$$
\tau_0^{(1)} < \tau_0^{(2)} < \tau_1^{(1)} < \tau_1^{(2)} < \cdots < \tau_k^{(1)} < \tau_{k+1}^{(1)} < \tau_k^{(2)}. \tag{15}
$$

The behaviors in Remarks (a)–(c) describe the situation of a stability switch as τ increases: a pair of characteristic roots cross the imaginary axis to the right at $\tau = \tau_0^{(1)}$ and cross back to the left at $\tau = \tau_0^{(2)}$, so on and so forth, until for $\tau = \tau_k^{(1)}$ a pair of characteristic roots will cross to the right and remain to the right of the imaginary axis. Correspondingly, the HAM/TSP equilibrium P_2 will switch from being asymptotically stable for $\tau < \tau_0^{(1)}$ to being unstable for $\tau_0^{(1)} < \tau < \tau_0^{(2)}$, then to being asymptotically stable for $\tau_0^{(2)} < \tau_1^{(1)}$, and so on and so forth. Such a behavior of stability switch as τ increases is summarized in the following theorem. Similar behaviors have been observed in other biological models with time delays (Beretta and Kuang 2002; Beretta and Tang 2003; Beretta et al. 2006; Carletti and Beretta 2007; Tang and Zhou 2007; Crauste 2009).

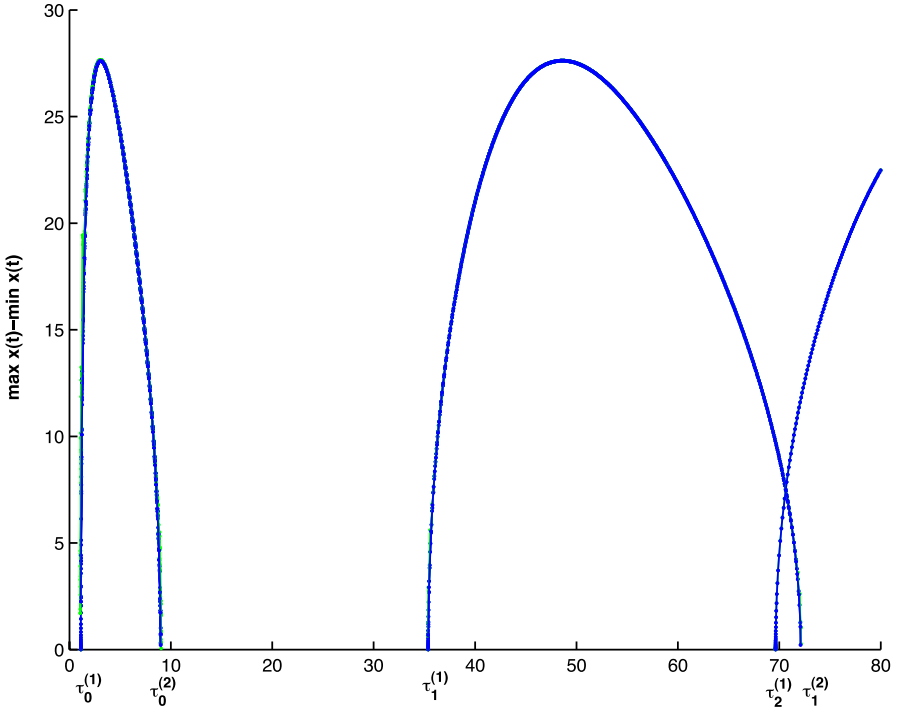

Fig. 2 A bifurcation diagram showing stability switch at HAM/TSP equilibrium P_2 and the global Hopf branches. Parameter values are given in (16)

Theorem 3.4 *Let $k \in \mathbb{N}$ be such that condition (15) holds. Then the HAM/TSP equilibrium P_2 is asymptotically stable if $0 \le \tau < \tau_0^{(1)}$ or $\tau_{i-1}^{(2)} < \tau < \tau_i^{(1)}$, $i = 1, 2, \ldots, k$; and P_2 is unstable if $\tau_{i-1}^{(1)} < \tau < \tau_{i-1}^{(2)}$, $i = 1, 2, \ldots, k$, or $\tau > \tau_k^{(1)}$.*

4 Global Hopf Branches and Multiple Stable Periodic Solutions

In the previous section, we have described the situation when Hopf bifurcations occur along two sequences of τ values, and the HAM/TSP equilibrium P_2 can switch between being asymptotically stable and being unstable for finitely many times. It is more interesting to investigate properties of the global Hopf branches that accompany such stability-switch phenomenon. Based on the remark before Theorem 3.4, as characteristic roots cross the imaginary axis in opposite directions at $\tau_i^{(1)}$ and $\tau_i^{(1)}$, we can have such a situation that

(1) all global Hopf branches are bounded for $i = 0, 1, 2, \ldots, k$;
(2) each global Hopf branch connects a pair of τ values $\tau_i^{(1)}$ and $\tau_i^{(1)}$, $i = 0, 1, 2, \ldots, k$; and
(3) periodic solutions on each Hopf branch are orbitally asymptotically stable, $i = 0, 1, 2, \ldots, k$.

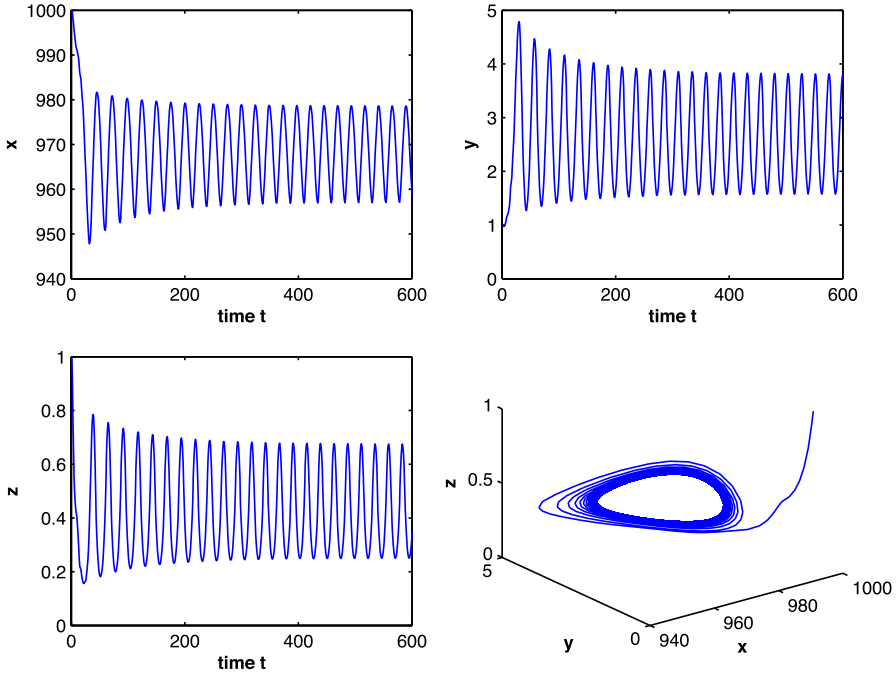

Fig. 3 A typical solution that converges to a stable periodic solution when $\tau = 6 \in (\tau_0^{(1)}, \tau_0^{(2)})$. The unit is cells/mm^3 on the vertical axes and days for time t

In the following, we will show numerical evidence that supports the phenomenon described in (1)–(3). The Hopf branches are computed using DDE32 in Matlab. Periodic solutions are simulated using Matlab.

In Figs. 2, 3, 4 and 5 we use the following set of parameter values:

$$\begin{aligned} &\lambda = 160 \text{ cells/mm}^3\text{/day}, \qquad \beta = 0.002 \text{ mm}^3\text{/cell/day}, \\ &\gamma = 0.2 \text{ mm}^3\text{/cells/day}, \qquad \mu = 0.2 \text{ mm}^3\text{/cells/day}, \\ &d_1 = 0.16 \text{ day}^{-1}, \qquad d_2 = 1.85 \text{ day}^{-1}, \qquad d_3 = 0.5 \text{ day}^{-1}. \end{aligned} \tag{16}$$

Solving (9) we obtain two positive roots, $\omega_1 = 0.1834$ and $\omega_2 = 0.0996$. From (13) we obtain two sequences of τ values (in days): $\tau_0^{(1)} = 1.224$, $\tau_1^{(1)} = 35.3819$, $\tau_2^{(1)} = 69.6413, \ldots$, and $\tau_0^{(2)} = 8.9928$, $\tau_1^{(2)} = 72.077, \ldots$. The first two global Hopf branches are shown in Fig. 2. We see that both branches are bounded and connect a pair of bifurcation values $(\tau_0^{(1)}, \tau_0^{(2)})$ and $(\tau_1^{(1)}, \tau_1^{(2)})$, respectively. The third Hopf branch, partially shown in Fig. 3, connects $(\tau_2^{(1)}, \tau_2^{(2)})$. Computing the Floquet multipliers on each Hopf branch, we can verify that periodic solutions are orbitally asymptotically stable. Also in Fig. 2, the HAM/TSP equilibrium P_2 corresponds to the zero solution. We can verify that P_2 is stable for $\tau \in (0, \tau_0^{(1)}) \cup (\tau_0^{(2)}, \tau_1^{(1)})$ and is unstable

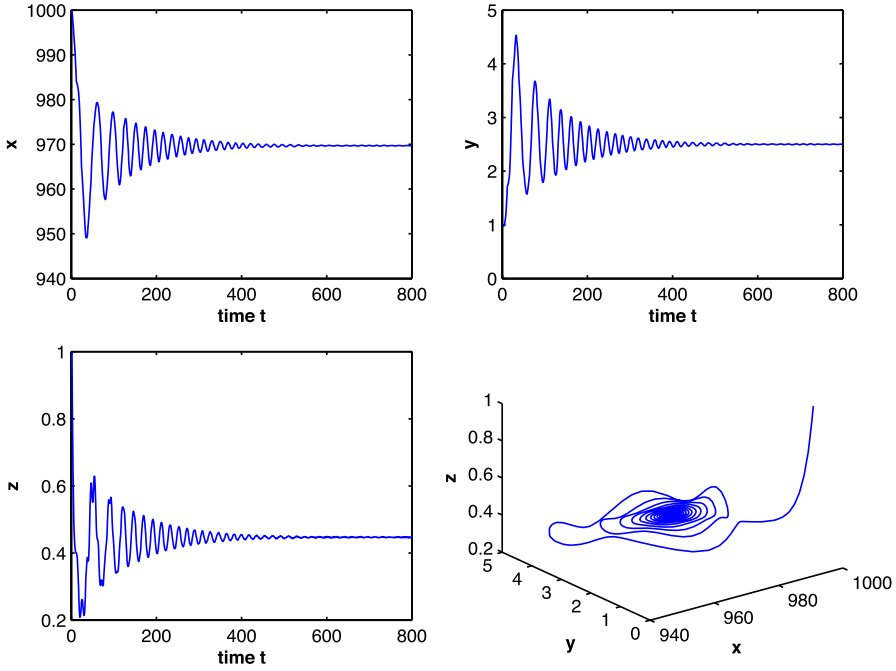

Fig. 4 A typical solution that converges to the stable HAM/TSP equilibrium P_3 when $\tau = 15 \in (\tau_0^{(2)}, \tau_1^{(1)})$. Parameter values are given in (16)

for $\tau \in (\tau_0^{(1)}, \tau_0^{(2)}) \cup (\tau_1^{(1)}, +\infty)$, due to the overlap of the second and the third Hopf branches.

In Figs. 3 and 4, we show two typical solutions for τ in the instability interval $(\tau_0^{(1)}, \tau_0^{(2)})$ and the stability interval $(\tau_0^{(2)}, \tau_1^{(1)})$, respectively. The solution in Fig. 3 moves away from the unstable P_2 and converges to a stable periodic solution, while the solution in Fig. 4 converges to the stable equilibrium P_2.

An interesting behavior occurs for $\tau \in (\tau_2^{(1)}, \tau_1^{(2)})$ in which the second and the third Hopf branches overlap. This creates the coexistence of two stable periodic solutions. In Fig. 5 (a) and (b), we show two stable periodic solutions for the same τ value at $\tau = 70$. We observe that the two solutions differ in both amplitude and period.

To demonstrate that the coexistence of multiple stable periodic solutions can occur in model (1) for reasonable values of the delay τ, we choose a slightly different set of parameter values for Figs. 6, 7 and 8:

$$\begin{aligned} &\lambda = 160 \text{ cells/mm}^3\text{/day}, \qquad \beta = 0.002 \text{ mm}^3\text{/cell/day}, \\ &\gamma = 0.2, \text{ mm}^3\text{/cells/day}, \qquad \mu = 0.2 \text{ mm}^3\text{/cells/day}, \\ &d_1 = 0.16 \text{ day}^{-1}, \qquad d_2 = 1.85 \text{ day}^{-1}, \qquad d_3 = 0.44 \text{ day}^{-1}. \end{aligned} \tag{17}$$

We obtain $\omega_1 = 0.1887$, $\omega_2 = 0.0479$, and $\tau_0^{(1)} = 0.8407$, $\tau_1^{(1)} = 34.1379$, $\tau_2^{(1)} = 67.4351$, $\tau_3^{(1)} = 100.7324$, ..., and $\tau_0^{(2)} = 37.79810$, $\tau_1^{(2)} = 168.9540$, ... The

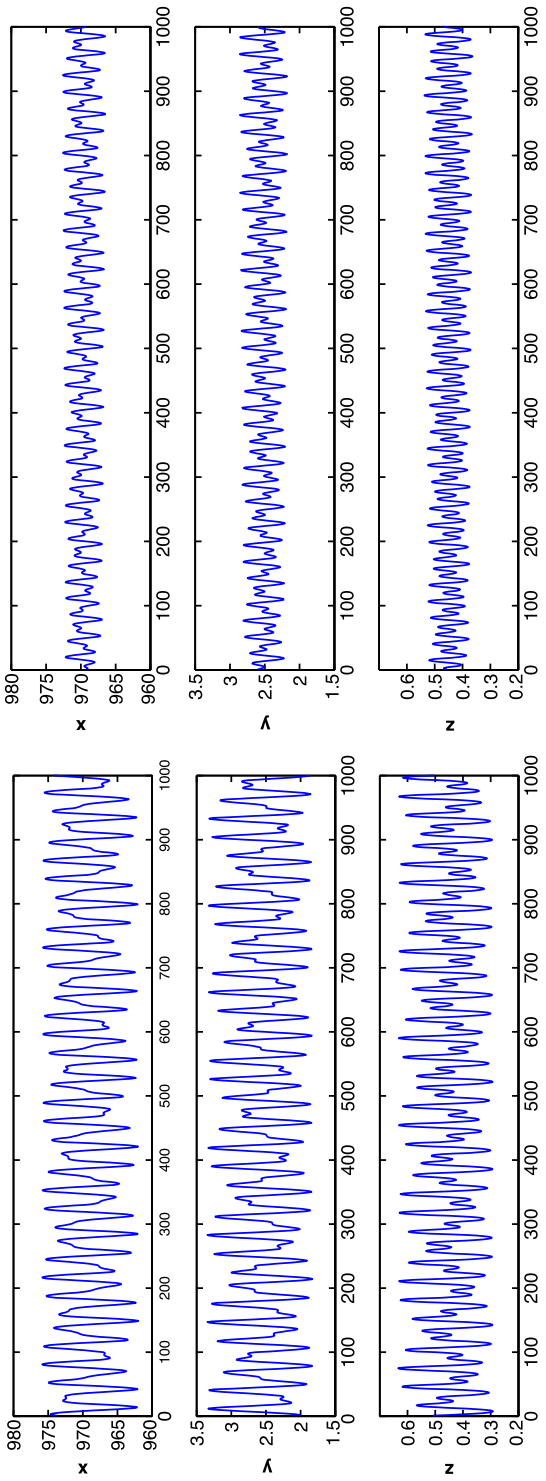

Fig. 5 Simulation results that show two coexisting stable periodic solutions for $\tau = 70 \in (\tau_2^{(1)}, \tau_1^{(2)})$. Parameter values are given in (16)

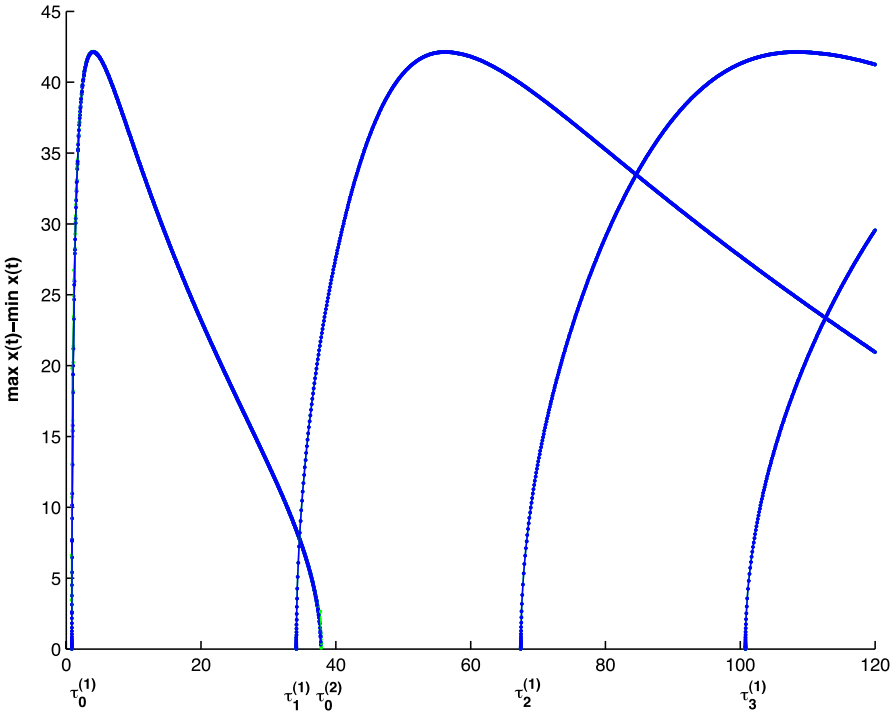

Fig. 6 A bifurcation diagram showing overlap of global Hopf branches. Parameter values are given in (17)

HAM/TSP equilibrium is unstable for $\tau > \tau_0^{(1)}$. We see in Fig. 6 that an overlap of global Hopf branches occurs for $\tau \in (34.1, 37.8)$, thus creating two coexisting stable periodic solutions for the same τ value, see Fig. 7. Further observe that, for $\tau \in (100, 200)$, we have an overlap of three Hopf branches, creating the possibility of coexistence of three stable periodic solutions. Two of such solutions are shown in Fig. 8. It is not hard to envision systems where any finite number of Hopf branches overlap and create coexistence of multiple stable periodic solutions.

5 Biological Implications and Further Discussions

Modelling study in the present paper, together with earlier HTLV-I modelling in the literature, suggests that the dynamic interaction between the HTLV-I infection and maintenance in the $CD4^+$ target-cell population and the CTL regulation of the HTLV-I proviral load can be very complex. The outcomes may include a stable steady state, a stable periodic oscillatory state, and several coexisting stable periodic oscillatory states. Mathematically speaking, when multiple stable periodic solutions coexist, the final outcome of the immune dynamics critically depends on the initial viral dosages. Clinical evidence seems to support such theoretical possibility. In Osame et al. (1990), it was shown that HTLV-I infection through blood transfusion is positively correlated with higher number of HAM/TSP patients. It was shown in Seto et al.

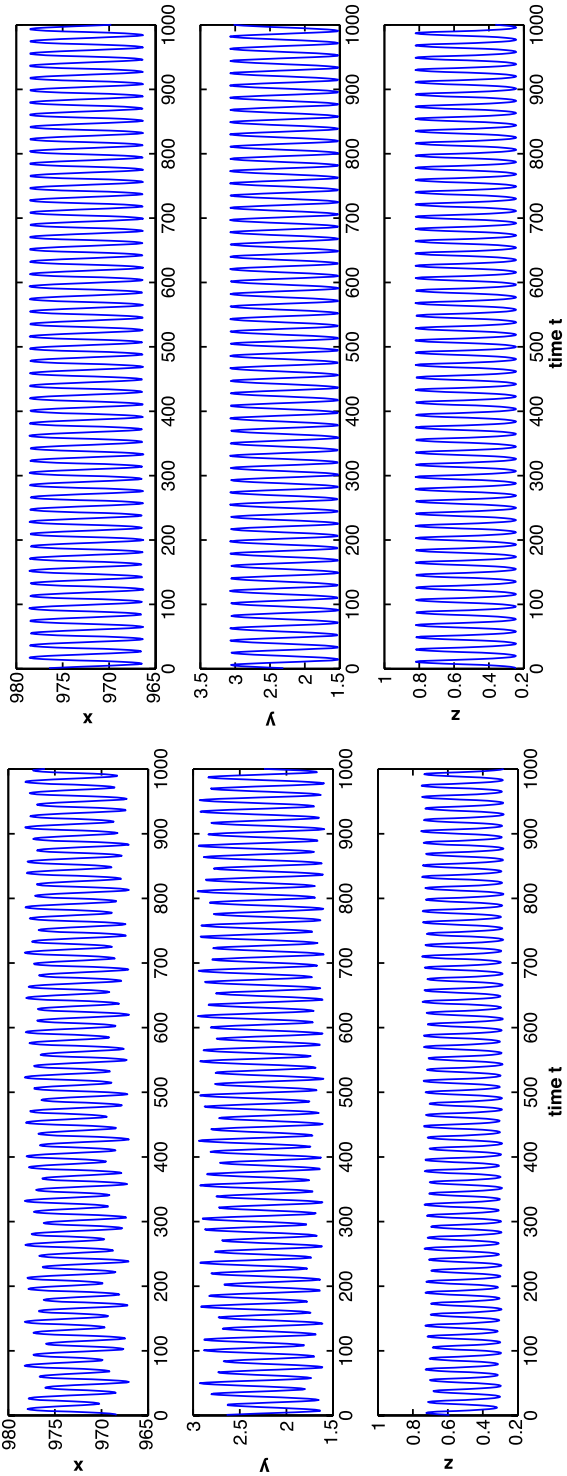

Fig. 7 Co-existence of two stable periodic solutions when $\tau = 35 \in (\tau_1^{(1)}, \tau_0^{(2)})$ in Fig. 6. Parameter values are given in (17)

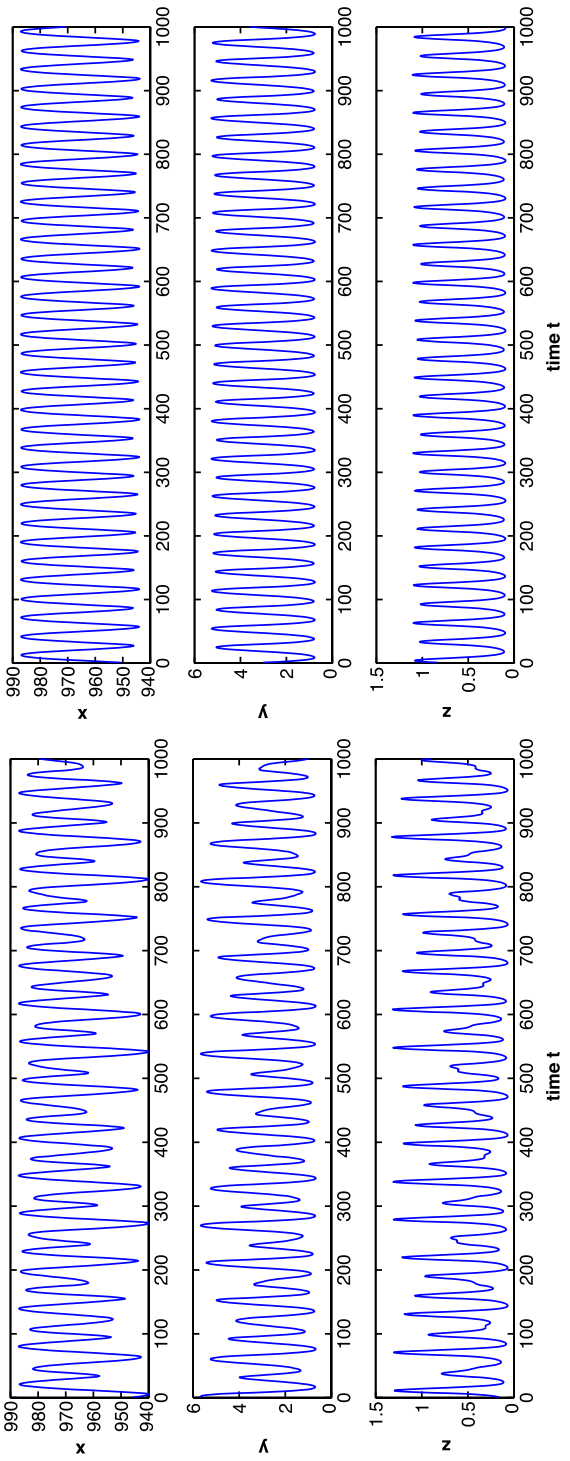

Fig. 8 Two of the three coexisting stable periodic solutions when $\tau = 115$. Parameter values are given in (17)

(1995) that chronic progressive myeloneuropathy can be developed in rats intraperitoneally inoculated with HTLV-I producing cells, and that a high dose of inoculation can significantly accelerate the disease onset. Coexistence of multiple stable periodic solutions also opens up the possibility of solutions to switch from the basin of attraction of one stable periodic solution to that of another, when the system is subjected to perturbations such as re-exposure to HTLV-I or medical interventions. In Wodarz et al. (1999), clinical evidence is shown that both CTL frequency and HTLV-I proviral load of a patient switch from a steady state to large-amplitude oscillations after anti-retroviral treatment. Understanding of theoretical possibilities revealed through mathematical modelling has practical implications for clinical diagnosis and for designing and administering medical treatment.

As shown in Figs. 2 and 4, for different values of the delay in CTL response, the system can stabilize at the positive equilibrium when the delay is small, or stabilize at a stable periodic oscillation when the delay is large. During the primary viral infection, the CTL response usually occurs a few days after the seroconversion (Koup et al. 1994), which is a long delay. During chronic infection phase, due to the presence of HTLV-I-specific memory cells, the CTL response can be much faster. Our results suggest that HTLV-I proviral load and HTLV-I-specific CTL frequency will likely to be oscillating during the primary infection, and tend to stabilize at a constant level during the chronic phase of the infection.

Acknowledgements The research supported in part by grants from the Natural Science and Engineering Research Council (NSERC) and Canada Foundation for Innovation (CFI). H. Shu acknowledges the financial support of a scholarship from the China Scholarship Council while visiting the University of Alberta. Both authors acknowledge the support from the Mathematics of Information Technology and Complex Systems (MITACS).

Appendix: Proof of Theorem 2.2

Proof of Theorem 2.2 (1) We assume that $R_0 \le 1$ and prove that the infection-free equilibrium P_0 is globally stable in the feasible region Γ. Consider a Lyapunov functional $L : \mathbb{R} \times \mathcal{C} \times \mathcal{C} \to \mathbb{R}$ given by

$$L(x(t), y_t, z_t) = y_t(0). \tag{A.1}$$

Here $y_t(s) = y(t+s)$, $z_t(s) = z(t+s)$ for $s \in [-\tau, 0]$, and thus $y(t) = y_t(0)$, $z(t) = z_t(0)$ in this notation. Calculating the time derivative of L along solutions of system (1), we obtain

$$\begin{aligned} L'|_{(1)} &= y'(t) = \beta x(t) y(t) - d_2 y(t) - \gamma y(t) z(t) \\ &\le y(t)(\beta x(t) - d_2) \le y(t)\left(\beta \frac{\lambda}{d_1} - d_2\right) = d_2 y(t)(R_0 - 1). \end{aligned}$$

Therefore, $R_0 \le 1$ ensures that $L'|_{(1)} \le 0$ for all $x(t)$, $y(t)$, $z(t) > 0$, and $L' = 0$ only if $y = 0$ or $R_0 = 1$. It can be verified that the maximal compact invariant set in $\{L'|_{(1)} = 0\}$ is the singleton P_0. By the LaSalle–Lyapunov Theorem (LaSalle and

Lefschetz 1961, Theorem 3.4.7), we conclude that P_0 is globally attractive in Γ if $R_0 \le 1$. Furthermore, it can be verified that P_0 is locally stable using the same proof as one for Corollary 5.3.1 in Hale and Lunel (1993). Therefore, P_0 is globally asymptotically stable in Γ when $R_0 \le 1$. □

Proof of Theorem 2.2 (2) and (3) The characteristic equation of the infection-free equilibrium P_0 is

$$(\xi + d_1)\left(\xi - \frac{\beta\lambda}{d_1} + d_2\right)(\xi + d_3) = 0. \tag{A.2}$$

The eigenvalues of (A.2) are $-d_1$, $\beta\lambda/d_1 - d_2$, and $-d_3$. If $R_0 > 1$, then $\beta\lambda/d_1 - d_2 = d_2(R_0 - 1) > 0$, and P_0 is unstable.

Now assume that $R_1 \le 1 < R_0$. We prove that the carrier equilibrium P_1 is globally stable. Let

$$g(u) = u - \ln u, \quad \text{for } u \in (0, +\infty).$$

Let $P_1 = (\bar{x}, \bar{y}, 0)$ be the carrier equilibrium with $\bar{x}$, $\bar{y}$ given in (5). Define a Lyapunov functional $V : \mathbb{R} \times \mathcal{C} \times \mathcal{C} \to \mathbb{R}$:

$$V(x(t), y_t, z_t) = \overline{x} g\left(\frac{x(t)}{\overline{x}}\right) + \overline{y} g\left(\frac{y_t(0)}{\overline{y}}\right) + \frac{\gamma}{\mu} z_t(0) + \gamma \int_{-\tau}^{0} y_t(\theta) z_t(\theta)\, d\theta. \tag{A.3}$$

Since $g : \mathbb{R}_+ \to \mathbb{R}$ has the global minimum at $u = 1$ and $g(1) = 1$, the Lyapunov functional V is positive definite with respect to P_1 in the interior of Γ. Calculating the time derivative of V along solutions of system (1), we obtain

$$\begin{aligned} V'|_{(1)} &= \lambda - d_1 x(t) - \lambda \frac{\bar{x}}{x(t)} + d_1 \bar{x} + \beta \bar{x} y(t) \\ &\quad - d_2 y(t) - \beta \overline{y} x(t) + d_2 \overline{y} + \gamma \overline{y} z(t) - \frac{\gamma d_3}{\mu} z(t). \end{aligned}$$

Using $\lambda = d_1 \bar{x} + \beta \bar{x} \bar{y}$ and $d_2 = \beta \overline{x}$, we obtain

$$\begin{aligned} V'|_{(1)} &= (d_1 \bar{x} + \beta \bar{x} \bar{y})\left(2 - \frac{x(t)}{\bar{x}} - \frac{\bar{x}}{x(t)}\right) + \gamma\left(\overline{y} - \frac{d_3}{\mu}\right) z(t) \\ &= (d_1 \bar{x} + \beta \bar{x} \bar{y})\left(2 - \frac{x(t)}{\bar{x}} - \frac{\bar{x}}{x(t)}\right) + \frac{\gamma(d_1\mu + \beta d_3)}{\beta\mu}(R_1 - 1) z(t) \\ &\le \frac{\gamma(d_1\mu + \beta d_3)}{\beta\mu}(R_1 - 1) z(t) \le 0, \quad \text{if } R_1 \le 1, \end{aligned} \tag{A.4}$$

since

$$\frac{x(t)}{\overline{x}} + \frac{\overline{x}}{x(t)} - 2 \ge 0.$$

Furthermore, $V' = 0$ implies that $x(t) = \bar{x}$ and $z(t) = 0$, and thus the maximal compact invariant set in the set where $V' = 0$ is the singleton $\{P_1\}$. Positive definiteness

of V with respect to P_1 and a similar argument as in the proof of Theorem 2.2 (1) imply that, when $R_1 \leq 1 < R_0$, P_1 is globally asymptotically stable in $\Gamma \setminus \{x\text{-axis}\}$. Along the invariant x-axis, solutions converge to the infection-free equilibrium P_0. This establishes Theorem 2.2 (2).

When $R_1 > 1$ and for $x(t) > 0$ such that $|x(0) - x_0|$ is sufficiently small, we have $V'|_{(1)} > 0$ from (A.4). Therefore, solutions in the interior of Γ sufficiently close to P_1 move away from P_1, and the carrier equilibrium P_1 is unstable by the Lyapunov instability theorem (Hale and Lunel 1993). The instability of the two boundary equilibria P_0 and P_1, together with the local behaviors of solutions near P_0 and P_1, implies that the isolated compact invariant sets on the boundary of Γ are the two equilibria $\{P_0\} \cup \{P_1\}$, and they both repel towards the interior of Γ. As a result, system (1) is uniformly persistent by the standard uniform persistence theory (e.g. Freedman et al. 1994, Theorem 4.3). This establishes Theorem 2.2 (3). □

References

Asquith, B., & Bangham, C. R. M. (2007). Quantifying HTLV-I dynamics. *Immunol. Cell Biol.*, *85*, 280–286.

Bangham, C. R. (2000). The immune response to HTLV-I. *Curr. Opin. Immunol.*, *12*, 397–402.

Bangham, C. R. M. (2003). The immune control and cell-to-cell spread of human T-lymphotropic virus type 1. *J. Gen. Virol.*, *84*, 3177–3189.

Beretta, E., Carletti, M. et al. (2006). Stability analysis of a mathematical model of the immune response with delays. In Y. Iwasa, K. Sato, & Y. Takeuchi (Eds.), *Mathematics for life science and medicine* (pp. 179–208). Berlin: Springer.

Beretta, E., & Kuang, Y. (2002). Geometric stability switch criteria in delay differential systems with delay dependent parameters. *SIAM J. Math. Anal.*, *33*, 1144–1165.

Beretta, E., & Tang, Y. (2003). Extension of a geometric stability switch criterion. *Funkcial. Ekvac.*, *46*, 337–361.

Burić, N., Mudrinic, M., & Vasović, N. (2001). Time delay in a basic model of the immune response. *Chaos Solitons Fractals*, *12*, 483–489.

Carletti, M., & Beretta, E. (2007). Numerical detection of instability regions for delay models with delay-dependent parameters. *J. Comput. Appl. Math.*, *205*, 835–848.

Clark, L. H., Schlosser, P. M., & Selgrade, J. F. (2003). Multiple stable periodic solutions in a model for hormonal control of the menstrual cycle. *Bull. Math. Biol.*, *65*, 157–173.

Crauste, F. (2009). Delay model of hematopoietic stem cell dynamics: asymptotic stability and stability switch. *Math. Model. Nat. Phenom.*, *4*, 28–47.

Freedman, H. I., Tang, M. X., & Ruan, S. G. (1994). Uniform persistence and flows near a closed positively invariant set. *J. Dyn. Differ. Equ.*, *6*, 583–600.

Gallo, R. C. (2005). History of the discoveries of the first human retroviruses: HTLV-1 and HTLV-2. *Oncogene*, *24*, 5926–5930.

Gomez-Acevedo, H., & Li, M. Y. (2002). Global dynamics of a mathematical model for HTLV-I infection of T cells. *Can. Appl. Math. Q.*, *10*, 71–86.

Gomez-Acevedo, H., Li, M. Y., & Jacobson, S. (2010). Multi-stability in a model for CTL response to HTLV-I infection and its consequences in HAM/TSP development and prevention. *Bull. Math. Biol.*, *72*, 681–696.

Gyllenberg, M., & Yan, P. (2009). Four limit cycles for a three-dimensional competitive Lotka–Volterra system with a heteroclinic cycle. *Comput. Math. Appl.*, *58*, 649–669.

Hale, J. K., & Lunel, S. V. (1993). *Introduction to functional differential equations*. New York: Springer.

Hofbauer, J., & So, J. W. (1990). Multiple limit cycles for predator–prey models. *Math. Biosci.*, *99*, 71–75.

Hofbauer, J., & So, J. W. (1994). Multiple limit cycles for three-dimensional Lotka–Volterra equations. *Appl. Math. Lett.*, *7*, 65–70.

Hollsberg, P., & Hafler, D. A. (1993). Pathogenesis of diseases induced by human lymphotropic virus type I infection. *N. Engl. J. Med.*, *328*, 1173–1182.

Jacobson, S. (2002). Immunopathogenesis of human T-cell lymphotropic virus type I associated neurologic disease. *J. Infect. Dis.*, *186*, S187–S192.

Koup, R. A., Safrit, J. T., et al. (1994). Temporal association of cellular immune responses with the initial control of viremia in primary human immunodeficiency virus type 1 syndrome. *J. Virol.*, *68*, 4650–4655.

Kubota, R., Osame, M., & Jacobson, S. (2000). Retrovirus: human T-cell lymphotropic virus type I associated diseases and immune dysfunction. In M. W. Cunningham & R. S. Fujinami (Eds.), *Effects of microbes on the immune system* (pp. 349–371). Philadelphia: Lippincott Williams & Wilkins.

Lang, J., & Li, M. Y. (2010). Stable and transient periodic oscillations in a mathematical model for CTL response to HTLV-I infection. Preprint.

LaSalle, J., & Lefschetz, S. (1961). *Stability by Liapunov's direct method*. New York: Academic Press.

Li, M. Y., & Shu, H. (2010). *Global dynamics of a mathematical model for HTLV-I infection of* $CD4^+$ *T cells with delayed CTL response*. Preprint.

Nowak, M. A., & May, R. M. (2000). *Virus dynamics: mathematical principles of immunology and virology*. Oxford: Oxford University Press.

Osame, M., Janssen, R., et al. (1990). Nationwide survey of HTLV-I-associated myelopathy in Japan: association with blood transfusion. *Ann. Neurol.*, *28*, 50–56.

Perelson, A. S., & Nelson, P. W. (1999). Mathematical analysis of HIV-I dynamics in vivo. *SIAM Rev.*, *41*, 3–44.

Pilyugin, S. S., & Waltman, P. (2003). Multiple limit cycles in the chemostat with variable yield. *Math. Biosci.*, *132*, 151–166.

Seto, K., Abe, M. et al. (1995). A rat model of HTLV-I infection: development of chronic progressive myeloneuropathy in seropositive WKAH rats and related apoptosis. *Acta Neuropathol.*, *89*, 483–490.

Tang, Y., & Zhou, L. (2007). Stability switch and Hopf bifurcation for a diffusive prey–predator system with delay. *J. Math. Anal. Appl.*, *334*, 1290–1307.

Wang, K., Wang, W., Pang, H., & Liu, X. (2007). Complex dynamic behavior in a viral model with delayed immune response. *Physica D*, *226*, 197–208.

Wodarz, D., & Bangham, C. R. M. (2000). Evolutionary dynamics of HTLV-I. *J. Mol. Evol.*, *50*, 448–455.

Wodarz, D., Nowak, M. A., & Bangham, C. R. M. (1999). The dynamics of HTLV-I and the CTL response. *Immunol. Today*, *20*, 220–227.